Push−Pull Molecules in the Gas Phase: Stark-Effect Measurements of the Permanent Dipole Moments of *p*-Aminobenzoic Acid in Its Ground and Electronically Excited States

D. M. Mitchell, P. J. Morgan, and D. W. Pratt*

Department of Chemistry, University of Pittsburgh, Pittsburgh, Pennsylvania 15260

Received: August 4, 2008; Revised Manuscript Received: October 4, 2008

Stark effect measurements of the permanent electric dipole moments of *p*-aminobenzoic acid (PABA) in the gas phase are reported based on studies of its fully resolved $S_1 \leftarrow S_0$ electronic spectrum in the presence of an electric field. Ground-state (S_0) PABA has $\mu = 3.3$ D, whereas excited-state (S_1) PABA has $\mu = 4.4$ D. Despite PABA's reputation as a "push−pull" molecule, the photon-induced change in both the magnitude and orientation of μ is relatively small. Possible reasons for this behavior are discussed.

Introduction

Knowledge of the permanent electric dipole moment of a molecule can give us a wealth of information. Among other things, it can allow us to determine a molecule's conformation.[1,2] Electric deflection experiments are currently being used to measure the ground-state dipole moments of biomolecules in the gas phase, and these values have been used to make conclusions about peptide motion and shape.[3,4] Recently, helix formation in alanine-based peptides was investigated; on the basis of dipole measurements, it was suggested that the peptides formed β-sheets in the gas phase, which was surprising as they usually form α-helices in solution.[4]

Dugourd and co-workers have also studied some smaller molecules, such as *p*-aminobenzoic acid (PABA).[5] PABA, shown in Figure 1, can be classified as a "push−pull" molecule, with two substituents, an amino group and a carboxyl group, that may donate or withdraw electron density to or from the benzene ring. PABA has been the focus of other gas phase studies,[6] including deflection studies of its dimer.[7,8]

High-resolution fluorescence excitation spectroscopy performed in the presence of an electric field is a powerful tool that allows us to determine the electric dipole moments of isolated molecules by tracking the Stark shifts of individual transitions.[9] Here, this technique has been applied to PABA. We measure both the ground- and excited-state permanent electric dipole moments of PABA in the gas phase. Comparison is made to the electric deflection results and also to aniline (AN).

Experimental Section

PABA (99% purity) was purchased from Sigma-Aldrich and used without further purification. To obtain vibrationally resolved LIF spectra, a 50/50 mixture of PABA and diatomaceous earth was heated to ∼130 °C, seeded into ∼2 kTorr of dry helium gas (>90% purity), and expanded through a 1 mm diameter orifice pulsed valve (General Valve Series 9), operating at 10 Hz, into a vacuum chamber (10^{-5} Torr). Diatomaceous earth was used in order to limit decomposition of PABA. The gaseous sample was then crossed 2 cm downstream with the output of a Quanta Ray Nd^{3+}:YAG (Model DCR-1A) pumped dye laser (Model PDL-1), using a mixture of Kiton Red and Rhodamine 590 dyes. Frequency doubling was done externally with a potassium dihydrogen phosphate (KDP) crystal. The visible portion of the laser output was filtered, leaving ultraviolet (UV) light with a spectral resolution of ∼1 cm^{-1}. A photomultiplier tube (EMI 9813QB), positioned at right angles to both the laser and molecular beams, was used to collect the fluorescence. The data were processed by a boxcar integrator (Stanford Research Systems) and recorded using Quick Data Acquisition software (version 1.0.5).

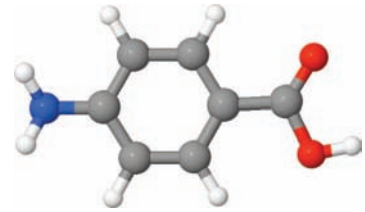

Figure 1. Structure of PABA.

Rotationally resolved experiments were performed using a molecular beam laser spectrometer, described elsewhere.[10] Briefly, the sample was heated to ∼190 °C, seeded in dry argon gas (>99% purity), and expanded into a vacuum through a 240-μm quartz nozzle. The molecular beam was skimmed 2 cm downstream with a 1 mm diameter skimmer and then crossed 15 cm downstream with the frequency-doubled output of the dye laser. Rhodamine 590 dye was used, and ∼1 mW of UV light was produced. Fluorescence was collected using spatially selective optics and detected by a photomultiplier tube (EMI 9813 QB) and photon counting system. An iodine absorption spectrum and relative frequency markers were simultaneously collected. All information was processed using the jba95 data acquisition system.[10] Absolute transition frequencies in the excitation spectrum were determined by comparison with the I_2 absorption spectrum (accuracy ≈ 30 MHz). The frequency markers were generated by a stabilized etalon with a free spectral range of 299.7520 ± 0.0005 MHz at the fundamental frequency of the dye. Fitting of the field-free spectrum was done using the jb95 least-squares fitting program.[11] The experimental setup of the Stark cell and general analysis of Stark spectra have been described elsewhere.[9]

The high-resolution spectra of PABA both in the presence and absence of an applied electric field are relatively weak; we presume that this is due to the decomposition of PABA upon heating (the fluorescence quantum yield is fairly high).[12] For

* To whom correspondence should be addressed. E-mail: pratt@pitt.edu.

10.1021/jp806950m CCC: $40.75
Published on Web 11/18/2008

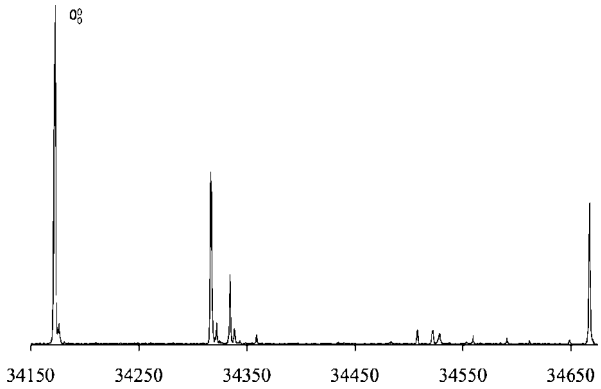

Figure 2. Low-resolution fluorescence excitation spectrum of PABA.

this reason, the intracavity frequency doubler in our modified Spectra-Physics 380D ring laser was replaced by a Wavetrain external frequency doubler, also manufactured by Spectra-Physics. UV power levels of ~1 mW were generated using the Kiton Red/Rhodamine 590 dye mixture and a BBO doubling crystal cut for 600 nm, a factor of 5 improvement over intracavity doubling in this frequency region. Details of the setup are provided elsewhere.[13]

Results

Figure 2 shows the vibrationally resolved fluorescence excitation spectrum (FES) of PABA. It is similar in many respects to the resonance-enhanced multiphoton ionization spectrum of laser-desorbed PABA taken by Meijer et al.[6] The electronic origin is the strongest band in both spectra, and their frequencies are very nearly the same. There is also extensive vibrational structure in both spectra. However, there are significant differences in both the frequencies and intensities of the observed vibronic bands in the two spectra. Possibly, these differences may be traced to the different sample preparation methods; some decomposition of PABA no doubt occurs at the high temperatures that were used in our experiment. But it is also possible that there are some differences in the quantum yields of fluorescence and ionization when exciting different vibronic bands.

The rotationally resolved FES spectrum of the origin band of PABA is shown in Figure 3. Lacking a strong Q-branch, it is a *b*-type spectrum, with the transition moment lying primarily along the *b*-axis. A simulation was created using rotational constants obtained from *ab initio* calculations,[14] and these constants were varied until there was good overall agreement between the experimental spectrum and the simulation. Figure 3 shows a portion of the simulation; each individual line in the simulation represents an individual $|J'K_a'K_c'\rangle \leftarrow |J''K_a''K_c''\rangle$ transition, and width has been added to reproduce the overall shape seen in the experiment. Over 100 transitions were assigned, and the best fit had an OMC (observed minus calculated standard deviation) of 2.4 MHz. The parameters obtained from this fit are given in Table 1. Rotational constants are in good agreement with calculations, with differences of 1% or less, less for the ground state.

The line width of individual transitions in the rotationally resolved origin band was fit using a Voigt profile comprised of a Gaussian line width of 18 MHz and a Lorentzian line width of ~30 MHz. The Gaussian component is due to Doppler broadening of the molecular beam; the Lorenztian component comes from lifetime broadening of the molecule. On the basis of our value of 30 MHz, the first excited-state of PABA has a lifetime around 5.3 ns. This is much longer than estimated by Meijer et al.,[6] who put the lifetime at a few hundred picoseconds. If the lifetime were that short, the lines seen in our experiment would be much broader, and we would not observe a resolved spectrum.

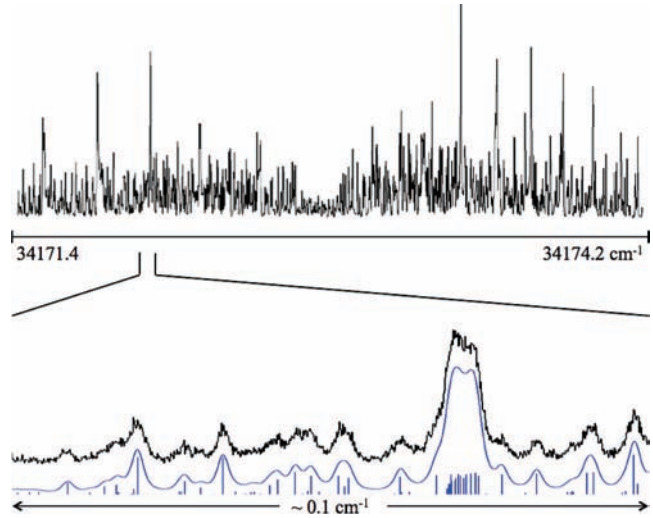

Figure 3. The field-free origin spectrum of PABA, occurring at 34172.8 cm^{-1}. Also shown in the bottom panel is a comparison of a small portion of the experimental spectrum (black trace) with two simulated spectra (blue trace), with and without a convoluted line shape function.

Application of an electric field causes transitions seen in the field-free spectrum to split and shift in frequency, as shown in Figure 4. The magnitudes of these shifts depend on both the field strength and dipole moment values. A special program[9] was used, in conjunction with jb95, to simulate and fit the experimental Stark spectra. This program carries out an exact diagonalization of truncated matrices and uses the following Hamiltonian

$$\hat{H} = \hat{H}_r + \hat{H}_e \quad (1)$$

The first term, $\hat{H}_r$, is the rigid-rotor Hamiltonian

$$\hat{H}_r = AJ_a^2 + BJ_b^2 + CJ_c^2 \quad (2)$$

and $\hat{H}_e$ is the Stark Hamiltonian

$$\hat{H}_e = -E_Z \sum_{g=a,b,c} \mu_g \varphi_{Z_g} \quad (3)$$

Here, A, B, and C are the rotational constants; J_a, J_b, and J_c are the projections of the angular momentum on the a, b, and c

TABLE 1: Experimental Inertial Parameters of PABA (Parameters Calculated at the MP2/6-31G and CIS/6-31G** Levels of Theory Have Also Been Included for Comparison)**

	experimental	calculated	% error
	S_0		
A (MHz)	3833.6 (1)	3821.3	0.3
B (MHz)	793.2 (1)	791.8	0.2
C (MHz)	657.8 (1)	656.3	0.2
ΔI (amu Å^2)	−0.66	−0.48	
	S_1		
A (MHz)	3692.3 (1)	3740.2	1.3
B (MHz)	795.5 (1)	804.7	1.2
C (MHz)	655.1 (1)	662.5	1.1
ΔI (amu Å^2)	−0.67	−0.32	
a/b/c	5/95/0		
origin (cm^{-1})	34172.8		

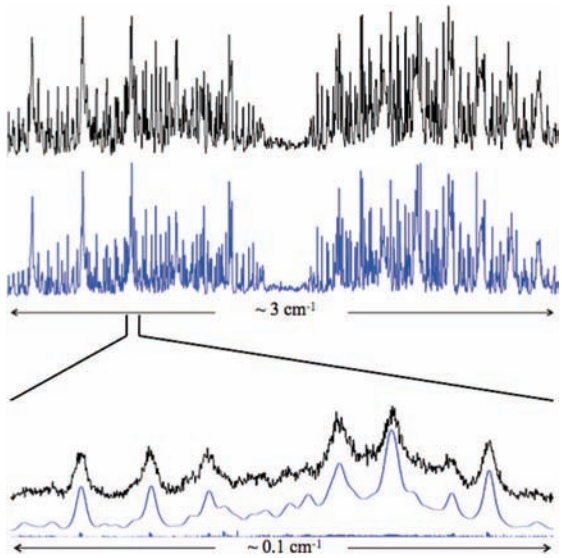

Figure 4. Origin spectrum of PABA at a calibrated electric field strength of 1184 V/cm. The black trace is the experimental spectrum, and the red trace is the simulated spectrum. The top portion shows the whole spectrum, while the bottom trace shows a close up of the highlighted section, again with and without a convoluted line shape function.

inertial axes; E_Z represents the electric field applied along the Z axis; μ_a, μ_b, and μ_c are the dipole moment components along each inertial axis; the direction cosines relating the laboratory and molecular frames are represented by ϕ. Other details have been described previously.[9] Recently, an improvement was made that more fully integrated the programs. One of the main features is a set of trackbars that allows the user to change the dipole moment components and "instantly" see the effects on the simulation.

Different transitions in the spectrum are affected differently by the application of the field. Certain transitions are more sensitive than others, both to the application of the electric field and to the different dipole moment components. This is illustrated in Figure 5. The positions of P- and R-branch lines with high K values, particularly those equal or nearly equal to J, are especially sensitive to μ_a, the positions of Q-branch lines are especially sensitive to μ_b, and the positions of the lines with $K_a = 0$ are especially sensitive to μ_c. Thus, to fit the spectrum in Figure 4 (and others at other field strengths), we first estimated μ_a, μ_b, and μ_c using *ab initio* methods, simulated an overall spectrum, and then focused on individual transitions that are most sensitive to the different dipole moment components to obtain a final fit of the observed spectrum. This is also shown in Figure 4. Typical OMC values of these fits are 7 MHz, substantially less than the line width.

Discussion

The value of μ_a obtained by electric deflection methods, 2.8 (2) D,[4] is in reasonable agreement with our directly measured value of 3.12 (8) D. This is not too surprising, since PABA is a near symmetric top and behaves well in an electric field.[5,15] In addition to the μ_a component, we are also able to measure the μ_b and μ_c components of the dipole moment, and we are able to measure all components in the electronically excited state. Thus, we also determine the orientation of the dipole moment in the molecular coordinate system and how it changes when the photon is absorbed.

The experimentally determined values of the dipole moment components are shown in Table 2. In general, the measured

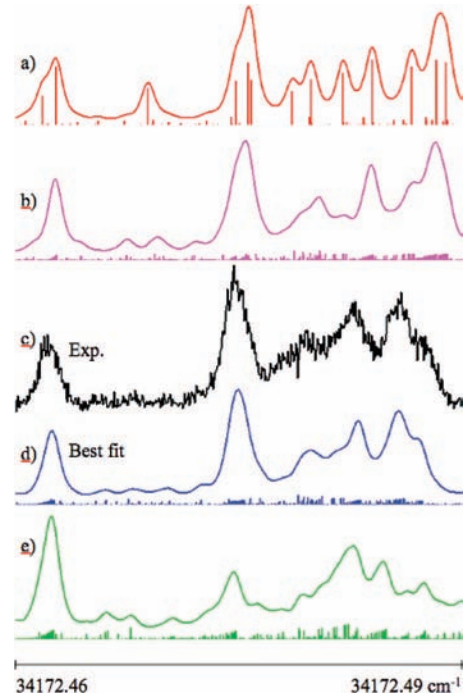

Figure 5. Several simulations, both with and without a convoluted line shape function, are compared to a portion of the Q-branch of the experimental spectrum to illustrate the dependence of the Stark spectra on the various dipole moment components. Simulation a is the zero-field spectrum, and traces b−e are at a calibrated field strength of 1184 V/cm. All simulations use the experimental rotational constants in Table 1. Simulation b assumes $\mu_a'' = 3.12$ and $\mu_a' = 4.21$ D, with the other components set to zero. Experimental spectrum c is shown for comparison. Below, simulation d is shown with $\mu_a'' = 3.12$, $\mu_a' = 4.21$, $\mu_b'' = 1.2$, $\mu_b' = 1.3$, $\mu_c'' = 0.0$, and $\mu_c' = 0.0$ D (the parameters obtained from our fits). Finally, simulation e was created with nonzero values of all dipole moment components, with $\mu_a'' = 3.12$, $\mu_a' = 4.21$, $\mu_b'' = 1.2$, $\mu_b' = 1.3$, $\mu_c'' = -1.26$, and $\mu_c' = -0.86$ D. The assumed values of μ_c are the calculated ones (Table 2).

values of the components of μ are substantially different from the calculated ones, with errors up to 30%. A special case is the out-of-plane component, μ_c. From our fits, μ_c was determined to be zero in both states, despite calculations predicting nonzero values; this has also been observed for AN.[9] A planar molecule would have $\mu_c = 0$. PABA, like AN, is relatively planar, except for the amino group which is positioned out of the plane. Calculations estimate the dihedral angle between the NH_2 and C_6H_4N planes to be ~28° in the ground state and ~20° in the excited state. In AN, the amino group undergoes an inversion motion that is fast relative to the rotational motion, resulting in

TABLE 2: Experimental Dipole Moment Values for PABA (Parameters Calculated at the MP2/6-31G and CIS/6-31G** Levels of Theory Have Also Been Included for Comparison)**

	experimental	calculated	% error
	S_0		
μ_a (D)	3.12 (8)	3.14	0.6
μ_b (D)	1.2 (2)	1.53	27.5
μ_c (D)	0.00 (1)	−1.26	
μ (D)	3.3 (2)	3.71	
	S_1		
μ_a (D)	4.21 (8)	4.12	2.1
μ_b (D)	1.3 (2)	1.53	17.7
μ_c (D)	0.00 (1)	−0.86	
μ (D)	4.4 (1)	4.48	

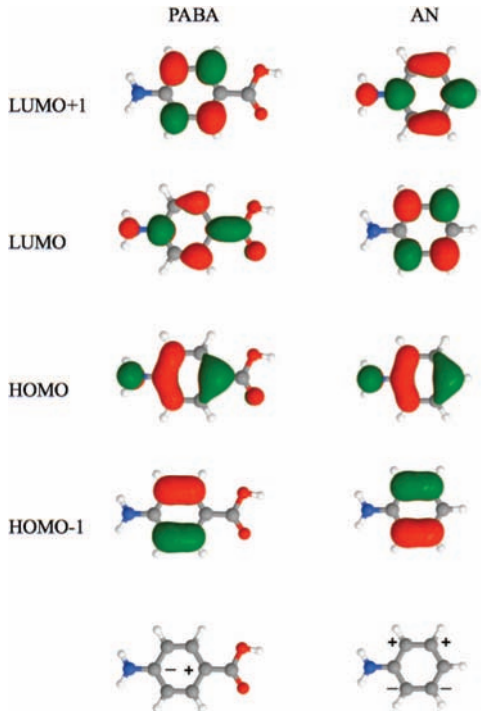

Figure 6. HOMO-1 (ϕ_2), HOMO (ϕ_3), LUMO (ϕ_4), and LUMO-1 (ϕ_5) orbitals of PABA and AN, as predicted by CIS/6-31G** calculations. The bottom portion shows the result of multiplication of the signs of the ϕ_3 and ϕ_4 orbitals, giving predicted transition moment orientations.

an average value of zero for μ_c.[9,17] We presume the same is true for PABA.

Figure 6 shows a comparison of the molecular orbitals of AN and PABA. The HOMO-1 (ϕ_2), HOMO (ϕ_3), LUMO (ϕ_4), and LUMO-1 (ϕ_5) orbitals are depicted. For PABA, the nodal pattern of the LUMO and LUMO+1 orbitals are reversed, relative to AN. On the basis of results observed for different conformations of alkyl benzenes,[18] this is not surprising; addition of the carboxyl group to AN breaks the symmetry of the molecule, rotating the positions of the nodal planes of the LUMO and LUMO+1 orbitals.

Calculations done at the CIS/6-31G** level of theory predict the S_1 state of AN to be a linear combination of one-electron excitations, $\Psi(S_1) = 0.28(\phi_2\phi_5) + 0.64(\phi_3\phi_4)$, with small contributions from other excitations. For PABA, calculations done at the same level of theory predict a similar combination: $\Psi(S_1) = 0.20(\phi_2\phi_5) + 0.65(\phi_3\phi_4)$, with small contributions from other excitations. The dominant excitation for both is HOMO to LUMO, and by multiplying the signs of these orbitals, we can predict the transition moment orientation of the excitation

TABLE 3: Comparison of Experimental Dipole Moment Values of PABA and AN

	PABA	AN[9,16]
	S_0	
μ_a (D)	3.12 (8)	1.129 (5)
μ_b (D)	1.2 (2)	0.00 (1)
μ_c (D)	0.00 (1)	0.00 (1)
μ (D)	3.3 (2)	1.129 (5)
	S_1	
$\Delta\mu_a$ (D)	1.1 (2)	1.67 (1)
$\Delta\mu_b$ (D)	0.1 (4)	0.00 (1)
$\Delta\mu_c$ (D)	0.00 (2)	0.00 (1)
$\Delta\mu$ (D)	1.1 (3)	1.672 (7)

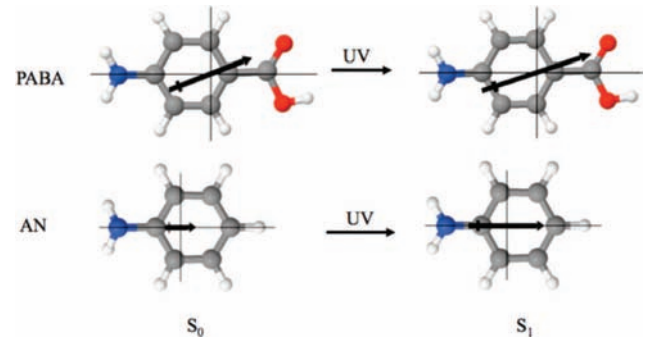

Figure 7. Arrows depicting the dipole moment magnitudes and directions of PABA and AN in both the ground and excited states.

in PABA. The result of this multiplication is depicted in the lower portion of Figure 6, and it shows that the predicted transition moment should lie parallel to the *a* axis for PABA. However, our experiments clearly show that the $S_1 \leftarrow S_0$ transition is *b* type, which means that the ordering of the molecular orbitals must follow that of AN. We conclude that the slight breaking of the symmetry by the carboxyl group must have a negligible effect on the positions of the nodal planes of the molecular orbitals of PABA.

The ground- and excited-state total dipole moments of PABA and AN are depicted in Figure 7. It should be noted that we do not obtain the direction of the dipole components from our fits; the directions shown in the figure are based on chemical intuition and the results of *ab initio* calculations. A comparison of the dipole moment values of PABA and AN is made in Table 3. The ground state μ_a dipole moment component of PABA, 3.12 (8) D, is larger than that of AN, 1.129 (5) D. This is due to the presence of the carboxyl group on PABA; −COOH groups are electron withdrawing (see Figure 6). Another measure of this effect is the proton affinity of the molecule in the gas phase, the energy released in the reaction $B + H^+ \rightarrow BH^+$. AN has a proton affinity of 877 kJ/mol, whereas that for PABA is somewhat less, 864.7 kJ/mol,[19] owing to the decrease in electron density on the $-NH_2$ group. Also notable is the magnitude of μ_b in PABA; the difference in the electron densities of the =O and −OH groups must be quite substantial, as μ makes a large angles with the *a* axis ($\sim 21°$ in S_0 and $\sim 18°$ in S_1).

The change in μ_a upon excitation is larger in AN than in PABA. Figure 8 shows electron density difference plots for AN and PABA, with light areas representing regions of electron density gain and dark areas representing regions of electron density loss.[20] In AN, it can be seen that charge is transferred from the amino group to the ring, resulting in the 1.67 D increase in μ_a. The increase in μ_a (1.1 D) in PABA is smaller than this. The electron density difference plot of PABA shows that the amino group donates electron density to the ring, as it does in AN, and that the carboxyl group also donates electron density to the ring. The donation made by the amino group increases μ_a relative to the ground state because it occurs in the same direction as the ground-state dipole. However, the donation of charge from the carboxyl group to the ring in PABA occurs in the opposite direction. Thus, the μ_a component still increases in PABA upon excitation, but the magnitude of the increase is less, relative to AN, due to the counteracting effect of the carboxyl group.

Conclusions

Rotationally resolved electronic spectroscopy has been performed in the presence of an electric field to determine the

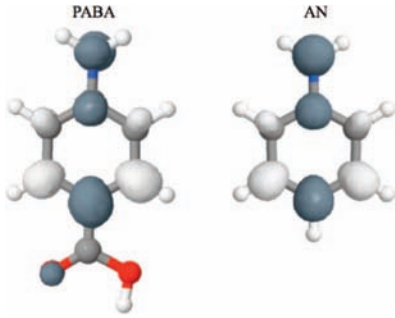

Figure 8. Electron density difference plots for AN and PABA. Light areas represent regions of electron gain, and dark areas represent regions of electron loss.

permanent electric dipole moment values for PABA in the gas phase in both its ground and excited states. The value of μ_a in the S_0 state is in reasonable agreement with electric deflection measurements taken by Dugourd et al.[5] The dipole moments of PABA have also been compared to those of AN. The addition of the carboxyl group withdraws electron density from the ring, resulting in an overall ground-state dipole moment that is larger than that of AN. There is also a significant μ_b component to the dipole in PABA; this indicates that there is a considerable electron density difference between the =O and −OH groups of the carboxyl. The change in μ_a of PABA upon excitation is slightly smaller in magnitude compared to that of AN, and the percent change is much smaller. Calculations suggest that both the amino and carboxyl substituents transfer some electron density back to the ring upon excitation. Because the donation of electron density from the carboxyl group occurs in a direction opposite to the dipole moment, the affect of the donation from the amino group is mitigated, resulting in a smaller change in μ_a than in AN.

Acknowledgment. We would like to thank D. F. Plusquellic his work on the Stark fitting program to further integrate it with the jb95 interface. We would also like to thank the Center for Molecular and Materials Simulations at the University of Pittsburgh for computing time, T. V. Nguyen for helpful discussions about using the Stark program, J. J. Grabowski for helpful discussions about proton affinities, and NSF for financial support (CHE-0615755).

References and Notes

(1) Reese, J. A.; Nguyen, T. V.; Korter, T. M.; Pratt, D. W. *J. Am. Chem. Soc.* **2004**, *126*, 11387.

(2) Nguyen, T. V.; Pratt, D. W. *J. Chem. Phys.* **2006**, *124*, 054317.

(3) Antoine, R.; Compagnon, I.; Rayane, D.; Broyer, M.; Dugourd, Ph.; Breaux, G.; Hagemeister, F. C.; Pippen, D.; Hudgins, R. R.; Jarrold, M. F. *J. Am. Chem. Soc.* **2002**, *124*, 6737.

(4) Dugourd, Ph.; Antoine, R.; Breaux, G.; Broyer, M.; Jarrold, M. F. *J. Am. Chem. Soc.* **2005**, *127*, 4675.

(5) Compagnon, I.; Antoine, R.; Rayane, D.; Broyer, M.; Dugourd, Ph. *J. Phys. Chem. A.* **2003**, *107*, 3036.

(6) Meijer, G.; de Vries, M. S.; Hunziker, H. E.; Wendt, H. R. *J. Chem. Phys.* **1990**, *92*, 7625.

(7) Compagnon, I.; Antoine, R.; Rayane, D.; Broyer, M.; Dugourd, Ph. *Phys. Rev. Lett.* **2002**, *89*, 253001.

(8) Abd El Rahim, M.; Antoine, R.; Arnaud, L.; Broyer, M.; Rayane, D.; Viard, A.; Dugourd, Ph. *Eur. Phys. J. D* **2005**, *34*, 15.

(9) Korter, T. M.; Borst, D. R.; Butler, C. J.; Pratt, D. W. *J. Am. Chem. Soc.* **2001**, *123*, 96.

(10) Majewski, W. A.; Pfanstiel, J. F.; Plusquellic, D. F.; Pratt, D. W. *Laser Techniques in Chemistry*; Wiley and Sons: New York, 1995; p 101.

(11) Plusquellic, D. F.; Suenram, R. D.; Maté, B.; Jensen, J. O.; Samuels, A. C. *J. Chem. Phys.* **2001**, *115*, 3057.

(12) Bello, J. M.; Hurtubise, R. J. *Appl. Spectrosc.* **1988**, *42*, 619.

(13) Mitchell, D. M. Ph.D. Thesis, University of Pittsburgh, 2008.

(14) Frisch, M. J.; Trucks, G. W.; Schlegel, H. B.; Scuseria, G. E.; Robb, M. A.; Cheeseman, J. R.; Montgomery, J. A., Jr.; Vreven, T.; Kudin, K. N.; Burant, J. C.; Millam, J. M.; Iyengar, S. S.; Tomasi, J.; Barone, V.; Mennucci, B.; Cossi, M.; Scalmani, G.; Rega, N.; Petersson, G. A.; Nakatsuji, H.; Hada, M.; Ehara, M.; Toyota, K.; Fukuda, R.; Hasegawa, J.; Ishida, M.; Nakajima, Y.; Honda, Y.; Kitao, O.; Nakai, H.; Klene, M.; Li, X.; Knox, J. E.; Hratchian, H. P.; Cross, J. B.; Bakken, V.; Adamo, C.; Jaramillo, J.; Gomperts, R.; Stratmann, R. E.; Yazyev, O.; Austin, A. J.; Cammi, R.; Pomelli, C.; Ochterski, J. W.; Ayala, P. Y.; Morokuma, K.; Voth, G. A.; Salvador, P.; Dannenberg, J. J.; Zakrzewski, V. G.; Dapprich, S.; Daniels, A. D.; Strain, M. C.; Farkas, O.; Malick, D. K.; Rabuck, A. D.; Raghavachari, K.; Foresman, J. B.; Ortiz, J. V.; Cui, Q.; Baboul, A. G.; Clifford, S.; Cioslowski, J.; Stefanov, B. B.; Liu, G.; Liashenko, A.; Piskorz, P.; Komaromi, I.; Martin, R. L.; Fox, D. J.; Keith, T.; Al-Laham, M. A.; Peng, C. Y.; Nanayakkara, A.; Challacombe, M.; Gill, P. M. W.; Johnson, B.; Chen, W.; Wong, M. W.; Gonzalez, C.; Pople, J. A. Gaussian 03, revision 6.0; Gaussian Inc.: Pittsburgh, PA, 2004.

(15) Abd El Rahim, M.; Antoine, R.; Broyer, M.; Rayane, D.; Dugourd, Ph. *J. Phys. Chem. A.* **2005**, *109*, 8507.

(16) Lister, D. G.; Tyler, J. K.; Høg, J. H.; Larsen, N. W. *J. Mol. Struct.* **1974**, *23*, 253.

(17) Hollas, J. M.; Howson, M. R.; Ridley, T.; Halonen, L. *Chem. Phys. Lett.* **1983**, *98*, 611.

(18) Kroemer, R. T.; Liedl, K. R.; Dickinson, J. A.; Robertson, E. G.; Simons, J. P.; Borst, D. R.; Pratt, D. W. *J. Am. Chem. Soc.* **1998**, *120*, 12573.

(19) Hunter, E. P.; Lias, S. G. *J. Phys. Chem. Ref. Data.* **1998**, *27*, 413.

(20) These plots were created by taking $(\phi_4^2-\phi_3^2)$ for AN and $(\phi_5^2-\phi_3^2)$ for PABA (since the calculated LUMO and LUMO+1 are reversed). Ideally, each plot would have been generated from a normalized linear combination of the HOMO to LUMO and the HOMO-1 to LUMO+1 excitations. However, since the orbital ordering was reversed for PABA, we could not rely on the calculated coefficients.

JP806950M